51. Mendell, J.R., Kissel, J.T., Amato, A.A., King, W., Signore, L., Prior, T.W., Sahenk, Z., Benson, S., McAndrew, PE., and Rice, R. 1995, N. Engl. J. Med., **333,** 832.
52. Bachrach, E., Li, S., Perez, A.L., Schienda, J., Liadaki, K., Volonski, J., Flint, A., Chamberlain, J., and Kunkel, L.M. 2004, Proc. Natl. Acad. Sci. U.S.A., **101,** 3581.
53. Bachrach, E., Perez, A.L., Choi, Y.H., Illigens, B.M., Jun, S.J., del Nido, P., McGowan, F.X., Li, S., Flint, A., Chamberlain, J., and Kunkel, L.M. 2006, Muscle Nerve, **34,** 44.
54. Benchaouir, R., Rameau, P., Decraene, C., Dreyfus, P., Israeli, D., Pietu, G., Danos, O., and Garcia, L. 2004, Exp. Cell Res., **294,** 254.
55. Israeli, D., Benchaouir, R., Ziaei, S., Rameau, P., Gruszczynski, C., Peltekian, E., Danos, O., and Garcia, L. 2004, J. Cell Physiol., **201,** 409.

JPSA
Japan Poultry Science Association

http://www.jstage.jst.go.jp/browse/jpsa
doi:10.2141/jpsa.46.95

Expression Pattern of *WWP1* in Muscular Dystrophic and Normal Chickens

Hirokazu Matsumoto[1], Hideaki Maruse[1], Shinji Sasazaki[1], Akira Fujiwara[2], Shin'ichi Takeda[3], Nobutsune Ichihara[4,5], Tateki Kikuchi[3], Fumio Mukai[1] and Hideyuki Mannen[1]

[1] Laboratory of Animal Breeding and Genetics, Graduate School of Agricultural Science, Kobe University, Kobe 657-8501, Japan
[2] Laboratory Animal Research Station, Nippon Institute for Biological Science, Kobuchisawa 408-0041, Japan
[3] Department of Molecular Therapy and of [4] Animal Models for Human Disease, National Institute of Neuroscience, NCNP, Kodaira, Tokyo 182-8502, Japan
[5] Department of Anatomy I, School of veterinary medicine, Azabu University, Fuchinobe, Sagamihara, Kanagawa 229-8501, Japan

The WW domain containing E3 ubiquitin protein ligase 1 (WWP1) is classified into one of ubiquitin ligases which play an important role in ubiquitin-proteasome pathway. Previously, we identified the *WWP1* gene as a candidate gene of chicken muscular dystrophy by linkage analysis and sequence comparison. However, the mechanism causing pathological changes and underlaying gene function remains elucidated. In the present study, we analyzed the *WWP1* gene expression in various muscles and tissues of normal chickens, and compared with those from muscular dystrophic chickens. Two mRNA isoforms were detected in all tissues examined and revealed almost equal expression level. The *WWP1* expression of dystrophic chickens was decreased in almost all skeletal muscles including unaffected muscles. These data indicate that there might not be a causal relationship between the alteration of *WWP1* expression level and the severity of muscular dystrophy.

Key words: chicken, expression analysis, fast twitch muscle fiber, muscular dystrophy, WWP1

J. Poult. Sci., 46: 95-99, 2009

Introduction

The WW domain containing E3 ubiquitin protein ligase 1 (*WWP1*) is classified into an ubiquitin ligase (E3) which plays an important role in ubiquitin-proteasome pathway (UPP) to degrade unneeded or damaged proteins (Scheffner and Staub, 2007). E3 recognizes and catalyzes ubiquitin (Ub) conjugation to specific protein substrates (Liu, 2004). Comparative genome analysis reveals few genes encoding E1, tens of E2 encoding genes and hundreds of E3 encoding genes (Semple *et al.*, 2003).

The *WWP1* gene is classified into HECT (homologous to the E6-AP carboxyl terminus)-type E3 which possesses one C2 domain, multiple WW domains and one HECT domain (Pirozzi *et al.*, 1997; Flasza *et al.*, 2002). The C 2 domain binds to the cellular membranes in a Ca^{2+}-dependent manner (Plant *et al.*, 1997) and mediates interactions with other proteins (Plant *et al.*, 2000; von Poser *et al.*, 2000; Augustine, 2001). The WW domain has two conserved tryptophan residues and binds proline-rich region (Sudol *et al.*, 1985). HECT domain, similar to E2s structurally, has a cysteine residue as an active center that transfers the activated Ub from E2 onto first itself, and then onto its substrates (Jackson *et al.*, 2000).

The muscular dystrophies are the group of inherited diseases with progressive weakness and degeneration of skeletal muscle (Partridge, 1991). It is well known that abnormalities of muscle proteins linking sarcolemma and basal lamina lead to cause muscular dystrophies (Lisi and Cohn, 2007), but there are a number of muscular dystrophies and related diseases of which causes are still unknown. We identified *WWP1* gene as a candidate responsible for the chicken muscular dystrophy by the linkage analysis (Matsumoto *et al.*, 2007) and the sequence comparison between normal and dystrophic chickens (Matsumoto *et al.*, 2008). The R441Q missense mutation was found in *WWP1* gene to cause the phenotype of muscular dystrophy.

The WWP1s of human (Flasza *et al.*, 2002; Komuro *et al.*, 2004), mouse (Dallas *et al.*, 2006) and *C. elegans* (Huang *et al.*, 2000) were intensively studied and known

Received: October 10, 2008, Accepted: December 24, 2008
Correspondence: Dr. H. Mannen, Graduate School of Agricultural Science, Kobe University, Kobe 657-8501, Japan.
(E-mail: mannen@kobe-u.ac.jp)

that the *WWP1* gene is expressed ubiquitously, but strongly in liver, bone marrow, testis and skeletal muscles (Flasza *et al.*, 2002; Komuro *et al.*, 2004). In chicken, however, the *WWP1* expression has not been studied. The expression analysis of *WWP1* gene is important since it was reported that altered expression of known responsible gene could lead dystrophic phenotype (Smythe and Rando, 2006).

In this study, we analyzed the mRNA expression of *WWP1* in various skeletal muscles and other tissues of normal and dystrophic chickens by using Northern blotting and reverse transcription (RT)-PCR analysis to know the differences in the general expression pattern between them.

Materials and Methods

Chickens

A two-month-old dystrophic chicken (New Hampshire: NH-413) and an age-matched normal chicken (White Leghorn: WL-F) were used in this study. The New Hampshire (NH-413) strain is a homozygous dystrophic line introduced from University of California, Davis to Japan in 1976 (Kondo *et al.*, 1982). The disease in this strain is transmitted co-dominantly by a single gene, but the phenotype is modified by other background genes (Kikuchi *et al.*, 1981, 1987; Wilson *et al.*, 1979). The White Leghorn (WL-F) strain was established in 1970s, and maintained as closed colony in the Nippon Institute of Biological Science in Yamanashi, Japan. This study was carried out according to the guidelines of Animal Experimentation of Kobe University.

Expression analysis

For Northern blotting, mRNAs were isolated from *M. pectoralis superficialis* (PS), *M. tensor fascia lata* (TFL), *M. biceps femoris* (BF), *M. triceps surae* (TS), *M. peroneus longus* (PL), heart (H), brain (B), liver (L), kidney (K) and whole embryo (E) with PolyATtract mRNA Isolation kit (Promega, Madison, WI, USA). The 2μg of mRNAs, which were measured with NanoDrop ND-1000 spectrophotometer (NanoDrop Technologies, Wilmington, DE, USA), were resolved by 1.2% agarose gel electrophoresis in the presence of formaldehyde and blotted on to Hybond-N+membrane (GE Healthcare Bio-Sciences AB, Uppsala, Sweden). The mRNAs were visualized using digoxigenin (DIG) reagents, and kits for non-radioactive nucleic acid labeling and detection system (Roche Diagnostics, Basel, Switzerland) according to the procedure specified by the manufacturer excepting that the washing was done with 4×SCC 0.1% SDS at room temperature for 10 min, 4×SCC 0.1% SDS at 40°C for 8 min and then 2×SCC 0.1% SDS at 40°C for 8 min twice. The DIG-labeled DNA probes were prepared by PCR using DIG-dUTP using pectorals cDNA sample of a WL-F strain female as a template. The primers applied in this procedure were 5′-tccctcataaatgttgaaagcagaca-3′ (WWP1p-F), 5′-gtaataacccaaggtaatatgtaaac-3′ (WWP1 p-R) (NM_001012554), 5′-ccgtgtgccaacccccaatgt ctctg-3′ (GAPDHp-F) and 5′ -cagtttctatcagcctctcccacctc- 3′ (GAPDHp-R) (NM_204305). The PCR was done for 35 cycles at 94°C for 30 sec, 55°C for 30 sec, 72°C for 30 sec (*WWP1*) and for 35 cycles at 94°C for 30 sec, 63°C for 30 sec, 72°C for 30 sec (*GAPDH*) using TaKaRa Ex Taq® Hot Start Version (Takara Bio Inc., Tokyo, Japan). Quantitative analysis was performed with Scion Image (Scion Corporation, Frederick, MD, USA).

In order to analyze mRNA expression of *WWP1* gene in the PS, *M. anterior latissimus dorsi* (ALD) and H, RT-PCR method was applied. The concentration of cDNA derived from these muscles was calculated by NanoDrop ND-1000 (NanoDrop Technologies) and commeasurable cDNAs were used as template. The primers applied were 5′-attaggaagagccactgtagact-3′ (WWP1r-F) and 5′-tctgttgattgaggttctgctgt-3′ (WWP1r-R) (NM_001012554). The PCR was done for 35 and 40 cycles at 94°C for 30 sec, 56°C for 30 sec, 72°C for 30 sec using TaKaRa Ex Taq® Hot Start Version (Takara Bio Inc.).

Histology

The PS, ALD and H were snap-frozen in liquid nitrogen-cooled isopentane and sectioned in a cryostat (Leica Microsystems Japan, Tokyo, Japan). The histopathology was made by hematoxylin-eosin staining (HE) method (Kikuchi *et al.*, 1981).

Results

The mRNA expression of *WWP1* gene was detected by Northern blotting in various muscles and other tissues of normal and muscular dystrophic chickens (Fig. 1). Two bands were detected in all tissues examined, and revealed almost equally expression level in any muscles and tissues observed.

In the PS, BF, TS, PL, B and K, *WWP1* gene was strongly expressed in normal than in dystrophic chickens (Fig. 1). *GAPDH* was used as an internal control of *WWP 1* expression analysis. In TFL, L and E, similar *WWP1* expression level was observed between two phenotypes (Fig. 1).

RT-PCR analysis indicated that *WWP1* gene was expressed in slow tonic ALD, not only in PS and H of both phenotypes (Fig. 2A). Figure 2B shows histopathological changes in PS, ALD and H of normal and dystrophic chickens. The pathological findings in dystrophic PS were characterized by the degenerating fibers with many vacuoles in cytoplasm, the fatty infiltration into connective tissue, and the proliferation of nuclei within muscle fibers with large variation in sizes. However, no such lesions were observed in ALD and H from age-matched dystrophic chickens (Fig. 2B).

Discussion

Northern blotting with *WWP1* specific probe detected two bands in all tissues and muscles examined (Fig. 1). Northern blot analysis of *WWP1* expression in human tissues also exhibited two bands (Mosser *et al.*, 1998), and RT-PCR analysis showed that human *WWP1* gene had at

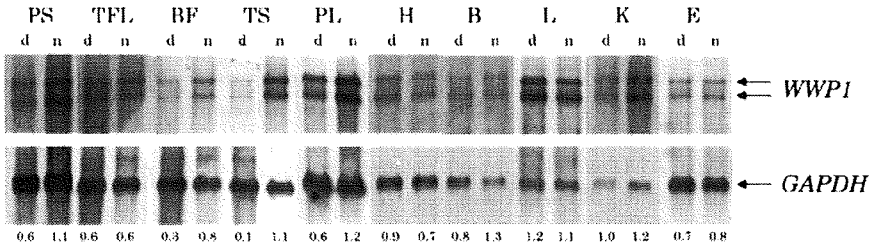

Fig. 1. **Expression of chicken *WWP1* in various tissues.**
A *WWP1* cDNA probe was used to detect *WWP1* mRNA transcripts by Northern blotting using blots containing 2μg of mRNAs from chicken muscles or various other tissues. *M. pectoralis superficialis* (PS), *M. tensor fascia lata* (TFL), *M. biceps femoris* (BF), *M. triceps surae* (TS), *M. peroneus longus* (PL), heart (H), brain (B), liver (L), kidney (K) and embryo (E) were analyzed. A doublet band is detected at variable levels in all tissues. "d" indicates mRNAs from dystrophic chickens. "n" indicates mRNAs from normal chickens. The numbers below the *GAPDH* bands represent the relative ratios of *WWP1/GAPDH*.

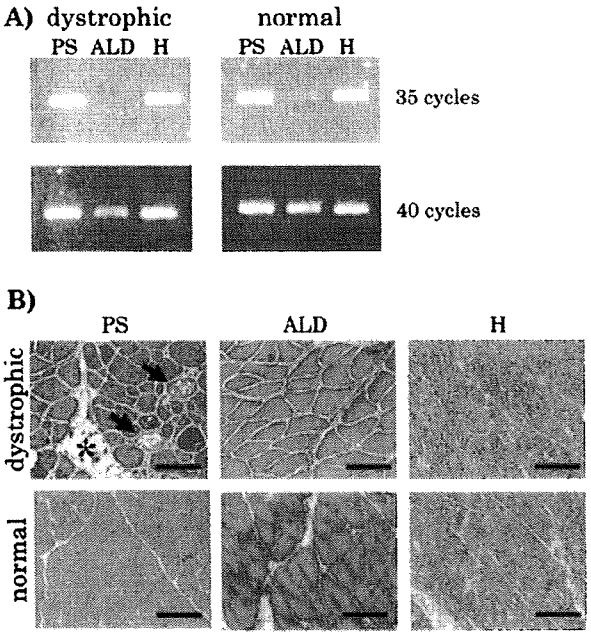

Fig. 2. **RT-PCR detection of *WWP1* gene and histological analysis for three representative muscle types.**
M. pectoralis superficialis (PS), *M. anterior latissimus dorsi* (ALD) and heart (H) expressed *WWP1* less in muscular dystrophic chicken, but only dystrophic PS was severely harmed. A) Expression of *WWP1* in PS, ALD and H was analyzed by RT-PCR method. PCR was performed for 35 or 40 cycles. B) The PS, ALD and H of dystrophic (NH-413) and normal (WL-F) chickens were analyzed with HE staining. Vacuoles (arrows) and fatty infiltration (asterisk) are observed in PS of dystrophic chickens. It is also remarkable that, in dystrophic PS, many muscle fibers have many nuclei in cytoplasm and vary widely in size. These pathological features are not observed in ALD and H of dystrophic chicken. Scale bar=120μm.

least six mRNA isoforms synthesized through the alternative splicing, two of which were strongly expressed and commonly observed in various tissues (Flasza *et al.*, 2002). The mRNA doublet bands of chicken *WWP1* by Northern blot analysis might be equivalent to two bands of human tissues, while a single band was observed by RT-PCR analysis in chicken (Fig. 2A), suggesting that the amplified region does not include alternative spliced site. Flasza *et al.* (2002) also mentioned that the relative ratio of these isoforms from human *WWP1* varied in a tissue-specific manner, but the doublet bands of chicken *WWP1* were expressed almost equally in all tissues examined.

The *WWP1* gene expression in *M. pectoralis superficialis* (PS) of dystrophic chicken was less than that of normal chicken (Fig. 1). The PS of chicken is a fast twitch muscle composed of two types of fast twitch fibers (aW and bW). TFL, BF, TS and PL muscles from wing and leg are mixed muscles co-existing fast twitch (aW and bW) with slow twitch fibers (bR) in a mosaic pattern (Ashmore and Doerr, 1971a), except that the ALD and *M. adductor magnus* are composed of slow tonic fibers (ST) innervated multiply (Ashmore *et al.*, 1978; Kikuchi *et al.*, 1986). In chicken muscular dystrophy, fast twitch fibers are initially and most severely affected, while slow twitch and slow tonic muscles persist relatively harmless throughout the life span (Ashmore and Doerr, 1971b; Barnard *et al.*, 1982). The *WWP1* expression in dystrophic BF, TS and PL showed a similar downward trend as observed in dystrophic PS (Fig. 1). These data indicate that there might not be a causal relationship between the alteration of *WWP1* expression level and the severity of muscular dystrophy, since not only affected muscles but unaffected ones exhibited the same pattern. Moreover, the alteration of *WWP1* expression level was observed in other unaffected tissues, such as B and K, which reinforces our hypothesis that the alteration of *WWP1* expression levels

does not link directly to the dystrophic phenotype (Fig. 1).

To assess the genetic influence of mutant *WWP1* upon chicken muscular dystrophy, we examined *WWP1* gene expression and histological changes in three distinct muscle types, PS as a fast twitch type, ALD as a slow tonic type, and H as a different type of muscle. RT-PCR was applied to this study since ALD was not enough quantity of mRNA for Northern blotting. The *WWP1* mRNA expression was confirmed in all muscles examined (Fig. 2 A).

Figure 2B shows HE stained sections of PS, ALD and H from normal and dystrophic chicken. The dystrophic PS was severely affected, while ALD and heart of dystrophic chicken remained relatively intact (Fig. 2B) as described in a previous study (Kikuchi *et al.*, 1981). The *WWP1* was expressed even in unaffected muscles and the downward alteration of *WWP1* expression was observed commonly in almost all dystrophic muscles examined (Figs. 1, 2). The observation suggests that the alteration of *WWP1* might not be the cause of the pathological change in chicken muscular dystrophy. Hence, the mutation identified previously (Matsumoto *et al.*, 2008) might play a crucial role in leading the onset of chicken muscular dystrophy. The detected mutation lay between WW domains, highly conserved region among tetrapods (Matsumoto *et al.*, 2008), which has been predicted as substrate binding region (Pirozzi *et al.*, 1997; Flasza *et al.*, 2002). This suggests that mutated *WWP1* could not recognize its substrates.

Many HECT-type E3s with WW domains including *WWP1* regulate membrane proteins (Chen and Matesic, 2007). Therefore, aberrant regulation of membrane protein may lead the onset of chicken muscular dystrophy. For example, *WWP1* could bind to β-dystroglycan, which is one of important muscle proteins consisting of membrane (Pirozzi *et al.*, 1997). Abnormal glycosylation of α-dystroglycan in chicken muscular dystrophy has been reported (Saito *et al.*, 2005). Furthermore, the fact that some E3s can recognize sugar chain (Yoshida *et al.*, 2002, 2003; Lederkremer and Gliskman, 2005) leads to the hypothesis that mutated *WWP1* might not be able to recognize the sugar chain of α-dystroglycan to regulate the glycosylated molecules, and that insufficiently glycosylated α-dystroglycan accumulates and causes the disease.

In the present study, we analyzed the mRNA expression of *WWP1* in various skeletal muscles and other tissues of normal and dystrophic chickens. The results suggest that *WWP1* expression level lowered in dystrophic phenotype is not directly related to the cause of disease in chicken muscular dystrophy, whereas mutated *WWP1* does not function normally to cause the onset of chicken muscular dystrophy.

Acknowledgments

This work was supported in part by Grant-in-Aid for Scientific Research (C), no. 19580338, and the Global COE Program "Global Center for Education and Research in Integrative Membrane Biology" (A-8) from the Ministry of Education, Science, Sports and Research on Nervous and Mental Disorders (16B-2, 19A-7) from the Japanese Ministry of Health, Labor and Welfare.

References

Ashmore CR and Doerr L. Comparative aspects of muscle fiber types in different species. Experimental Neurology, 31: 408-418. 1971a.

Ashmore CR and Doerr L. Postnatal development of fiber types in normal and dystrophic skeletal muscle of the chick. Experimental Neurology, 30: 431-446. 1971b.

Ashmore CR, Kikuchi T and Doerr L. Some observations on the innervation patterns of different fiber types of chick muscle. Experimental Neurology, 58: 272-284. 1978.

Augustine GJ. How does calcium trigger neurotransmitter release? Current Opinion in Neurobiology, 11: 320-326. 2001.

Barnard EA, Lyles JM, and Pizzey JA. Fibre types in chicken skeletal muscles and their changes in muscular dystrophy. The Journal of Physiology, 331: 333-354. 1982.

Chen C and Matesic LE. The Nedd4-like family of E3 ubiquitin ligases and cancer. Cancer Metastasis Reviews, 3-4: 587-604. 2007.

Dallas CJ, Marc NW, Mohamed O, Jochen GH, Melvin JG and Laurie HG. Regulation of Adult Bone Mass by the Zinc Finger Adapter Protein Schnurri-3. Science, 312: 1223-1227. 2006.

Flasza M, Gorman P, Roylance R, Canfield AE and Baron M. Alternative Splicing Determines the Domain Structure of WWP1, a Nedd4 Family Protein. Biochemical and Biophysical Research Communications, 290: 431-437. 2002.

Huang K, Johnson KD, Petcherski AG, Vandergon T, Mosser EA, Copeland NG, Jenkins NA, Kimble J and Bresnick EH. A HECT domain ubiquitin ligase closely related to the mammalian protein WWP1 is essential for Caenorhabditis elegans embryogenesis. Gene, 252: 137-145. 2000.

Jackson PK, Eldridge AG, Freed E, Furstenthal L, Hsu JY, Kaiser BK and Reimann JDR. The lore of the RINGs: substrate recognition and catalysis by ubiquitin ligases. Trends in Cell Biology, 10: 429-439. 2000.

Kikuchi T, Akiba T and Ashmore CR. Conversion of muscle fiber types in regenerating chicken muscles following cross-reinnervation. Acta Neuropathologica, 71: 197-206. 1986.

Kikuchi T, Ishiura S, Nonaka I and Ebashi S. Genetic heterozygous carriers in hereditary muscular dystrophy of chickens. Tohoku Journal of Agriculture Research, 32: 14-26. 1981.

Kikuchi T, Moriya H, Matuzani T, Katoh M and Takeda S. The development of laboratory animal science for the study of human muscular and nervous diseases in Japan. Congenital Anomalies, 27: 447-462. 1987.

Komuro A, Imamura T, Saitoh M, Yoshida Y, Yamori T, Miyazono K and Miyazawa K. Negative regulation of transforming growth factor-beta (TGF-beta) signaling by WW domain-containing protein 1 (WWP1). Oncogene, 23: 6914-6923. 2004.

Kondo K, Kikuchi T and Mizutani M. Breeding of the chicken as an animal model for muscular dystrophy. In: Muscular Dystrophy (Ebashi S ed.), pp. 19-24. Tokyo University

Press. Tokyo. 1982.
Lederkremer GZ and Glickman MH. A window of opportunity: timing protein degradation by trimming of sugars and ubiquitins. Trends in Biochemical Sciences, 30: 297-303. 2005.
Lisi MT and Cohn RD. Congenital muscular dystrophies: new aspects of an expanding group of disorders. Biochimica et Biophysica Acta, 1772: 159-172. 2007.
Liu YC. Ubiquitin ligases and the immune response. Annual Review of Immunology, 22: 81-127. 2004.
Matsumoto H, Maruse H, Yoshizawa K, Sasazaki S, Fujiwara A, Kikuchi T, Ichihara N, Mukai F and Mannen H. Pinpointing the candidate region for muscular dystrophy in chickens with an abnormal muscle gene. Animal Science Journal, 78: 476-483. 2007.
Matsumoto H, Maruse H, Inaba Y, Yoshizawa K, Sasazaki S, Fujiwara A, Nishibori M, Nakamura A, Takeda S, Ichihara N, Kikuchi T, Mukai F and Mannen H. The ubiquitin ligase gene (WWP1) is responsible for the chicken muscular dystrophy. FEBS Letters, 582: 2212-2218. 2008.
Mosser EA, Kasanov JD, Forsberg EC, Kay BK, Ney PA and Bresnick EH. Physical and functional interactions between the transactivation domain of the hematopoietic transcription factor NF-E2 and WW domains. Biochemistry, 37: 13686-13695. 1998.
Partridge T. Animal models of muscular dystrophy: what can they teach us? Neuropathology and Applied Neurobiology, 17: 353-363. 1991.
Pirozzi G, McConnell SJ, Uveges AJ, Carter JM, Sparksi AB, Kayi BK and Fowlkes DM. Identification of Novel Human WW Domain-containing Proteins by Cloning of Ligand Targets. The Journal of Biological Chemistry, 272: 14611-14616. 1997.
Plant PJ, Lafont F, Lecat S, Verkade P, Simons K and Rotin D. Apical membrane targeting of Nedd4 is mediated by an association of its C2 domain with annexin XIIIb. The Journal of Cell Biology, 149: 1473-1484. 2000.
Plant PJ, Yeger H, Staub O, Howard P and Rotin D. The C2 domain of the ubiquitin protein ligase Nedd4 mediates Ca^{2+}-dependent plasma membrane localization. The Journal of Biological Chemistry, 272: 32329-32336. 1997.
Saito F, Blank M, Schroder J, Manya H, Shimizu T, Campbell KP, Endo T, Mizutani M, Kroger S and Matsumura K. Aberrant glycosylation of a-dystroglycan causes defective binding of laminin in the muscle of chicken muscular dystrophy. FEBS Letters, 579: 2359-2363. 2005.
Scheffner M and Staub O. HECT E3s and human disease. BMC Biochemistry, 8 Suppl 1: S6. 2007.
Semple CA, RIKEN GER Group and GSL Members. The comparative proteomics of ubiquitination in mouse. Genome Research, 13: 1389-1394. 2003.
Smythe GM and Rando TA. Altered caveolin-3 expression disrupts PI (3) kinase signaling leading to death of cultured muscle cells. Experimental cell research, 312: 2816-2825. 2006.
Sudol M, Chen HI, Bougeret C, Einbond A and Bork P. Characterization of a novel protein-binding module: the WW domain. FEBS Letters, 369: 67-71. 1985.
von Poser C, Zhang JZ, Mineo C, Ding W, Ying Y, Sudhof TC and Anderson RG. Synaptotagmin regulation of coated pit assembly. The Journal of Biological Chemistry, 275: 30916-30924. 2000.
Wilson BW, Randall WR, Patterson GT and Entrikin RK. Major physiologic and histochemical characteristics of inherited dystrophy of the chicken. Annals of the New York Academy of Sciences, 317: 224-246. 1979.
Yoshida Y, Chiba T, Tokunaga F, Kawasaki H, Iwai K, Suzuki T, Ito Y, Matsuoka K, Yoshida M, Tanaka K and Tai T. E 3 ubiquitin ligase that recognizes sugar chains. Nature, 418: 438-442. 2002.
Yoshida Y, Tokunaga F, Chiba T, Iwai K, Tanaka K and Tai T. Fbs2 is a new member of the E3 ubiquitin ligase family that recognizes sugar chains. The Journal of Biological Chemistry, 278: 43877-43884. 2003.

ABSTRACT: Duchenne muscular dystrophy (DMD) is a devastating muscle disorder that is characterized by progressive muscle necrosis, fibrosis, and fatty infiltration. To examine the temporospatial pathological changes, a noninvasive evaluation method such as magnetic resonance imaging (MRI) is needed. The aim of this study was to precisely assess muscle necrosis and inflammation based on a sequence of T2-weighted imaging (T2WI), gadolinium-enhanced imaging, and selective fat suppression, chemical shift selective T2-weighted imaging (CHESS-T2WI), on a 3.0-Tesla MRI unit in 3-month-old and 7-year-old dogs with canine X-linked muscular dystrophy ($CXMD_J$), a suitable animal model for DMD. The results show that CHESS-T2WI was more sensitive and useful from the early to late stages of $CXMD_J$ than T2WI or contrast enhancement imaging in the evaluation of muscle necrosis, because these latter sequences can be influenced by fatty infiltration or interstitial connective tissues.

Muscle Nerve **40:** 815–826, 2009

EVALUATION OF DYSTROPHIC DOG PATHOLOGY BY FAT-SUPPRESSED T2-WEIGHTED IMAGING

MASANORI KOBAYASHI, DVM,[1,2] AKINORI NAKAMURA, MD, PhD,[1] DAISUKE HASEGAWA, DVM, PhD,[2] MICHIO FUJITA, DVM, PhD,[2] HIROMITSU ORIMA, DVM, PhD,[2] and SHIN'ICHI TAKEDA, MD, PhD[1]

[1] Department of Molecular Therapy, National Institute of Neuroscience, NCNP, 4-1-1 Ogawa-higashi, Kodaira, Tokyo 187-8502, Japan
[2] Department of Veterinary Radiology, Nippon Veterinary and Life Science University, Tokyo, Japan

Accepted 23 March 2009

Duchenne muscular dystrophy (DMD) is a severe X-linked muscle disease characterized by progressive skeletal muscle atrophy and weakness.[1] DMD is caused by mutations in the *dystrophin* gene, which encodes the cytoskeletal protein dystrophin.[2] A loss of dystrophin accompanied by a deficiency of dystrophin–glycoprotein complex (DGC) from the sarcolemma leads to progressive degeneration of striated muscle.[3,4] In dystrophic skeletal muscles, muscle fiber necrosis with inflammation is followed by muscle regeneration, but the muscle is finally replaced by fibrous or fatty tissue.[5,6] For this devastating disorder, various therapeutic approaches, such as gene therapy, stem cell–based cell therapy, or pharmaceutical agents have been proposed and explored using various DMD animal models.

The X-linked muscular dystrophy (*mdx*) mouse and Golden Retriever muscular dystrophy (GRMD) dog are the most commonly used DMD animal models.[7,8] *mdx* mice show extensive necrosis followed by regeneration, but their phenotypes are milder than those of DMD due to the absence of apparent fibrosis and fatty infiltration.[7,9,10] The phenotypes of striated muscle in the GRMD dog are clinically and pathologically more similar to that of DMD,[8,11,12] but it is very difficult to maintain this animal model due to the severe phenotype. We have therefore established a Beagle-based colony of canine X-linked muscular dystrophy in Japan ($CXMD_J$).[13] We have found that the clinical and pathological findings in $CXMD_J$ are similar to but milder than those in GRMD.[14,15]

A method of noninvasive temporospatial assessment is required to investigate muscle involvement and, especially, to evaluate therapeutic

Abbreviations: ANOVA, analysis of variance; CE, contrast enhancement ratio; CHESS, chemical shift selective; CT, computed tomography; $CXMD_J$, canine X-linked muscular dystrophy in Japan; DGC, dystrophin–glycoprotein complex; DMD, Duchenne muscular dystrophy; EDL, extensor digitorum longus; FDS, flexor digitorum superficialis; FITC, fluorescein isothiocyanate; GC, gastrocnemius; Gd-DTPA, gadolinium diethylenetriamine pentaacetic acid; GMRD, Golden Retriever muscular dystrophy; MRI, magnetic resonance imaging; PCr, phosphocreatine; Pi, inorganic phosphate; ROI, region of interest; SNR, signal-to-noise ratio; STIR, short-tau inversion recovery; SI, signal intensity; TC, tibialis cranialis

Key words: chemical shift selective fat-suppressed T2-weighted imaging; Duchenne muscular dystrophy; dystrophic dog; magnetic resonance imaging; myopathy

Correspondence to: S. Takeda; e-mail: takeda@ncnp.go.jp

Published online 7 August 2009 in Wiley InterScience (www.interscience.wiley.com). DOI 10.1002/mus.21384

interventions. Computed tomography (CT), which shows high temporal and spatial resolution, has been used to detect selective muscle involvement, such as atrophy or fatty tissue replacement, in patients suffering from DMD,[16,17] but it requires ionizing radiation and has limited sensitivity for soft tissues.[18] Magnetic resonance imaging (MRI) produces high-resolution images with good contrast among soft tissues,[19] and therefore it has been used to evaluate skeletal muscle involvement in DMD[20] and in *mdx* mice.[21] In the early stages of dystrophy, the T1 relaxation time is prolonged due to muscle degeneration and regeneration together with an increase in muscle water concentration, and it is decreased owing to fat infiltration in the advanced stage.[22] As the main magnetic field increases, however, the capacity to differentiate tissues on the basis of T1 relaxation time may decrease.[23] On the other hand, the T2 relaxation time is prolonged in necrotic as well as fatty and connective tissue[19]; therefore, it can hardly distinguish necrosis from fat replacement or fibrosis during the dystrophic process. To selectively detect necrotic changes, MR contrast agents, such as gadolinium diethylenetriamine pentaacetic acid (Gd-DTPA), have been used extensively,[24–26] but these agents may also enhance blood vessels and the interstitium,[27] and may cause severe adverse effects, such as anaphylaxis,[28,29] which are critical for DMD patients. Thus, a safer imaging protocol is needed to distinguish necrotic lesions from fatty degeneration or fibrosis in the dystrophic skeletal muscle of DMD and $CXMD_J$.

To discriminate necrosis from fatty infiltration, one of the fat suppression sequences may be useful. As a fat suppression sequence, short-tau inversion recovery (STIR) MR imaging was used to detect muscle edema in DMD.[6] However, STIR suppresses the signal from any tissue or fluid that has a short T1 relaxation time, and therefore it does not selectively suppress the fat signal.[30,31] In contrast, chemical shift selective (CHESS) imaging, another fat suppression sequence, is a technique that selectively saturates fat magnetization by applying a 90° pulse matching with the fat resonance frequency and therefore leads to a highly selective suppression of fat signals. Moreover, the signal-to-noise ratio (SNR) of CHESS is better than that of STIR at a higher magnetic field. The sequence of CHESS combined with T2-weighted imaging (CHESS-T2WI) has been used to diagnose disorders such as lipomatous tumor or temporomandibular arthrosis.[32–34] The method, however, has not been applied to evaluation of the dystrophic changes seen in DMD or the animal models to date.

We, therefore, examined dystrophic dog muscle by CHESS-T2WI to determine whether this sequence is more useful for finding necrosis and inflammatory change than the conventional sequences of T2WI or contrast imaging.

METHODS

Animals. We used three 3-month-old normal male dogs (II-2308MN, II/III-3911MN, and II-4202MN), three littermate $CXMD_J$ male dogs (II-2302MA, II/III-3903MA, and II-4204MA), one 7-year-old normal male dog (00-174MN), and two 7-year-old $CXMD_J$ male dogs (II-C04MA and II-C12MA). II-2308MN, II-4202MN, II-2302MA, and II-4204MA were produced by mating a second-generation (G2) carrier female[13] and G2 affected male. II/III-3911MN and II/III-3903MA were the offspring of a G2 carrier female and a third-generation (G3) affected male. We obtained II-C04MA and II-C12MA by mating first-generation (G1) carrier female dogs and pure-bred normal male Beagles. 00-174MN was a pure-bred normal Beagle. All dogs were part of the breeding colony at the General Animal Research Facility, National Institute of Neuroscience, National Center of Neurology and Psychiatry (Tokyo, Japan), or the Chugai Research Institute for Medical Science, Inc. (Nagano, Japan). Ages, body weights, and serum creatine kinase values at the time of MRI of each dog are shown in Table 1. This study was carried out according to the guidelines provided by the Ethics Committee for the Treatment of Middle-sized Laboratory Animals of the National Center of Neurology and Psychiatry (Approval Nos. 18-02, 19-02, and 20-02).

MR Scanning and Image Analysis. General anesthesia was induced by an intravenous injection of thiopental sodium (20 mg/kg) before MRI scanning and was maintained by inhalation of isoflurane (2.0–3.0%). We examined lower leg muscles of these dogs by superconducting 3.0-Tesla MRI (Magnetom Trio; Siemens Medical Solutions, Erlangen, Germany) with a human extremity coil 18 cm in diameter. The MRI pulse sequences used were T1-weighted imaging (T1WI), T2WI, chemical shift selective T1-weighted imaging (CHESS-T1WI), CHESS-T2WI, gadolinium-enhanced T1-weighted imaging (Gd-T1WI), chemical shift selective gadolinium-enhanced T1-weighted imaging (CHESS-

Table 1. Clinical profiles of normal and dystrophic male dogs used in this study.

	Age (mo)	BW (kg)	Serum CK (IU/L)
Normal dogs			
II-2308MN	3	6.8	197
II/III-3911MN	3	7.7	318
II-4202MN	3	5.8	274
00-174MN	87	13.7	83
CXMDJ dogs			
II-2302MA	3	7.2	30,200
II/III-3903MA	3	6.6	22,300
II-4204MA	3	6.0	28,800
II-C04MA	85	11.5	6500
II-C12MA	94	11.6	1602

Body weight (BW) and serum creatine kinase (CK) values were measured on the day of MRI examination.

Gd-T1WI), and multi-echo T2WI for calculation of T2 relaxation time. In contrast-enhanced images, we injected 0.2 ml/kg of the gadolinium-based MR contrast agent Gd-DTPA (Magnevist; Bayer Schering Pharma, Berlin, Germany) for each sequence. In 3-month-old dogs, we scanned the images for 26 minutes, about 5 minutes after the intravenous injection. On the other hand, we took the images for 13 minutes in 7-year-old dogs at 25 minutes after the injection in order to minimize the risk of anesthesia on the cardiac involvement seen in advanced $CXMD_J$.[15] CHESS was employed to assess necrotic and inflammatory changes more precisely. The acquisition parameters for T1WI, CHESS-T1WI, Gd-T1WI, and CHESS-Gd-T1WI were based on spin echo: repetition time (TR)/echo time (TE) = 500/7.4 ms; slice thickness = 4 mm; field of view = 18 × 18 cm; matrix = 256 × 256; and NEX = 3. The parameters for T2WI and CHESS-T2WI were chosen based on fast spin echo: TR/TE = 4000/85 ms; slice thickness = 4 mm; field of view = 18 × 18 cm; matrix = 256 × 256; turbo-factor = 9; and NEX = 3. The parameters for multi-echo T2WI were selected based on spin echo: TR = 2000; TE = 11.8–118.0 (10 echoes); slice thickness = 4 mm; field of view = 28 × 28 cm; matrix = 256 × 256; and NEX = 2. We were able to clearly distinguish each lower leg muscle by each sequence. Representative cross-sectional images and anatomical locations of lower leg muscles by CHESS-T1WI in a 7-year-old normal dog are shown in Figure 1.

For quantitative analysis of the images, the manufacturer's software (Syngo MR2004A; Siemens Medical Solutions, Erlangen, Germany) was used. Flow artifacts were slight, but regions of interest (ROIs) were selected to avoid flow artifacts and large vessels as follows: three circular ROIs were picked in both right tibialis cranialis (Rt. TC) and extensor digitorum longus (Rt. EDL) muscles of the 3-month-old dogs. ROIs were also selected in the Rt. TC of the 7-year-old dogs and a normal dog. Then, T2 relaxation time or signal intensities (SIs) of CHESS-T1WI, CHESS-Gd-T1WI, and CHESS-T2WI were measured in these ROIs. Signal-to-noise ratios (SNRs) of each ROI were calculated by the equation: $SNR = SI/SD_{air}$, where SD_{air} was the standard deviation (SD) of background noise.[35] The contrast enhancement (CE) ratio was calculated using the SNR of CHESS-T1WI ($SNR_{precontrast}$) and SNR of CHESS-Gd-T1WI ($SNR_{postcontrast}$) by the following equation: $CE = SNR_{postcontrast}/SNR_{precontrast}$. We used the means of the quantitative values at three points of ROIs for statistical analysis.

Statistical Analysis. The T2 relaxation time, CE ratio, and SNR of CHESS-T2WI were evaluated using a one-way analysis of variance (ANOVA) to determine differences among the groups. When a significant difference was found with one-way ANOVA, intergroup comparisons were undertaken using Fisher's protected least significant difference test. All values are expressed as mean ± SE, and statistical significance was recognized at $P < 0.05$.

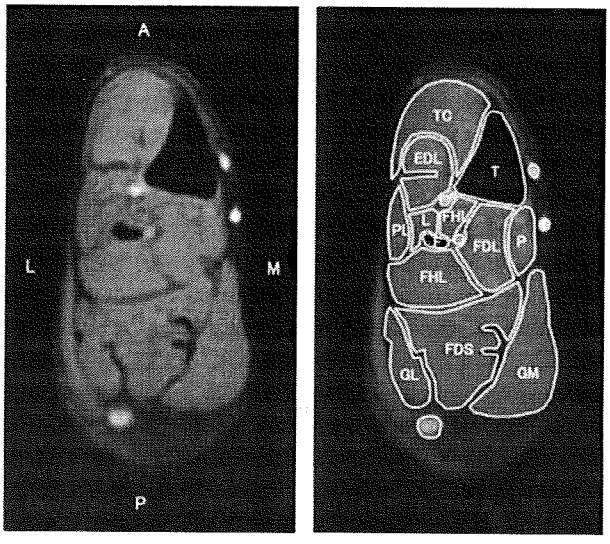

FIGURE 1. Cross-sectional images and anatomical orientation of right lower leg muscles of a 7-year-old normal dog in CHESS-T1WI. A 7-year-old normal dog (00-174MN) was used for this study. T, tibia; F, fibula; TC, tibialis cranialis; EDL, extensor digitorum longus; FHL, flexor hallucis longus; FDL, flexor digitorum longus; FDS, flexor digitorum superficialis; GM, gastrocnemius medialis; GL, gastrocnemius lateralis. A, anterior; P, posterior; L, lateral side; M, medial side.

Histopathology. We performed muscle biopsies of the right TC and right EDL on a 3-month-old normal dog (II-2308MN) and a $CXMD_J$ dog (II-2302MA), and right TC on a 7-year-old normal dog (00-174MN) and a $CXMD_J$ dog (II-C04MA) after MRI scanning. The muscle samples were snap-frozen in liquid nitrogen cooled by isopentane. Hematoxylin and eosin (H&E) staining was performed on serial 10-μm transverse cryostat sections. Anti-IgG immunofluorescence staining was performed on 6-μm serial cryostat sections incubated with fluorescein isothiocyanate (FITC)-conjugated polyclonal sheep anti-canine IgG (1:200; AbD Serotec, Oxford, UK) overnight. To examine fatty infiltration in the muscle, 6-μm serial frozen sections from normal and $CXMD_J$ dogs at 7 years of age were stained with oil red O.

RESULTS

MRI Findings of Lower Leg Muscles in 3-Month-Old Normal Dogs. First, we acquired muscle images of three 3-month-old normal dogs by T1WI, T2WI, CHESS-T1WI, CHESS-T2WI, Gd-T1WI, and CHESS-Gd-T1WI. Representative cross-sectional images of II-2308MN are shown in Figure 2A. In normal dogs, the lower leg muscles showed a homogeneous signal intensity in these sequences, but the muscles that contain mainly slow-twitch fibers, such as the gastrocnemius (GC) and flexor digitorum superficialis (FDS) (Fig. 2A, e and i), showed slight hyperintensity on T2WI and CHESS-T2WI when compared with muscles that contain mainly fast-twitch fibers such as TC and EDL (Fig. 2A, e and i). These findings were consistent with the previous T2 relaxation time study of rabbit muscles.[36] Gd-T1WI (data not shown) or CHESS-Gd-T1WI (Fig. 2A, g) showed homogeneous and slight enhancement when compared with T1WI (Fig. 2A, a) or CHESS-T1WI (Fig. 2A, c), respectively, in all normal dogs.

MRI Findings of Lower Leg Muscles in 3-Month-Old Dystrophic Dogs. Next, we tried to detect muscle involvement in three 3-month-old $CXMD_J$ dogs. Clinically, the dogs showed mild to moderate muscle atrophy and gait or mobility disturbance. These clinical findings are compatible with our previous study of $CXMD_J$dogs.[14] Representative cross-sectional images of II-2302MA are shown in Figure 2A.

All lower leg muscles of the three $CXMD_J$ showed no change on T1WI and CHESS-T1WI (Fig. 2A, b and d), but almost all lower leg muscles, especially EDL and GC, revealed remarkable hyperintensity on T2WI when compared with the images of normal dogs. We should note that the hyperintensity on TC was rather slight compared with that of the other lower leg muscles (Fig. 2A, f). We found that contrast agent uptake by Gd-T1WI (data not shown) or CHESS-Gd-T1WI (Fig. 2A, h) was increased in the areas where hyperintensity was recorded by T2WI. These findings suggest the necrotic and/or inflammatory changes that were shown in a previous study of *mdx* mice.[21] Hyperintensity was also clearly indicated by CHESS-T2WI in these regions, where hyperintensity on T2WI and contrast agent uptake in Gd-T1WI or CHESS-Gd-T1WI were noted (Fig. 2A, j).

Comparison of MR Signal Intensities of 3-Month-Old Normal and Dystrophic Dogs. To quantitatively evaluate MRI findings of three normal and three $CXMD_J$ dogs, we measured T2 relaxation time, CE based on comparison between SNR of CHESS-T1WI and CHESS-Gd-T1WI, and SNR of CHESS-T2WI. In TC, the T2 relaxation time of $CXMD_J$ dogs was significantly prolonged (49.8 $\pm$ 2.3 ms) when compared with that of normal dogs (39.9 $\pm$ 1.2 ms) ($P = 0.0004$). Moreover, T2 relaxation time of EDL was significantly prolonged in $CXMD_J$ (58.6 $\pm$ 3.1 ms) when compared with not only that in normal dogs (40.0 $\pm$ 0.5 ms) but also that of TC in $CXMD_J$ dogs ($P < 0.0001$ and $P = 0.0008$, respectively) (Fig. 2B, a).

Similarly, the effect of contrast enhancement in TC and EDL of $CXMD_J$ (1.659 $\pm$ 0.077 and 1.936 $\pm$ 0.127-fold) was significantly increased in comparison with that of normal dogs (1.511 $\pm$ 0.009 and 1.528 $\pm$ 0.015 fold) ($P = 0.0413$ and $P = 0.0002$, respectively), but the effect in TC of $CXMD_J$ was more prominent in EDL of $CXMD_J$ ($P = 0.0019$) (Fig. 2B, b).

In TC, the SNR of CHESS-T2WI was significantly increased in $CXMD_J$ (102.3 $\pm$ 12.1) when compared with that of normal dogs (70.0 $\pm$ 3.6) ($P = 0.0019$). Moreover, the SNR of CHESS-T2WI was significantly increased in EDL of $CXMD_J$ (146.0 $\pm$ 11.7) when compared with not only that of normal dogs (69.2 $\pm$ 2.9) but also that in TC of $CXMD_J$ dogs ($P < 0.0001$ and $P = 0.0003$, respectively), indicating EDL was more affected than TC in the early stage of $CXMD_J$ (Fig. 2B, c).

Histopathological Findings in Lower Leg Muscles of 3-month-old Normal and Dystrophic Dogs. To determine the relationship between MRI findings and

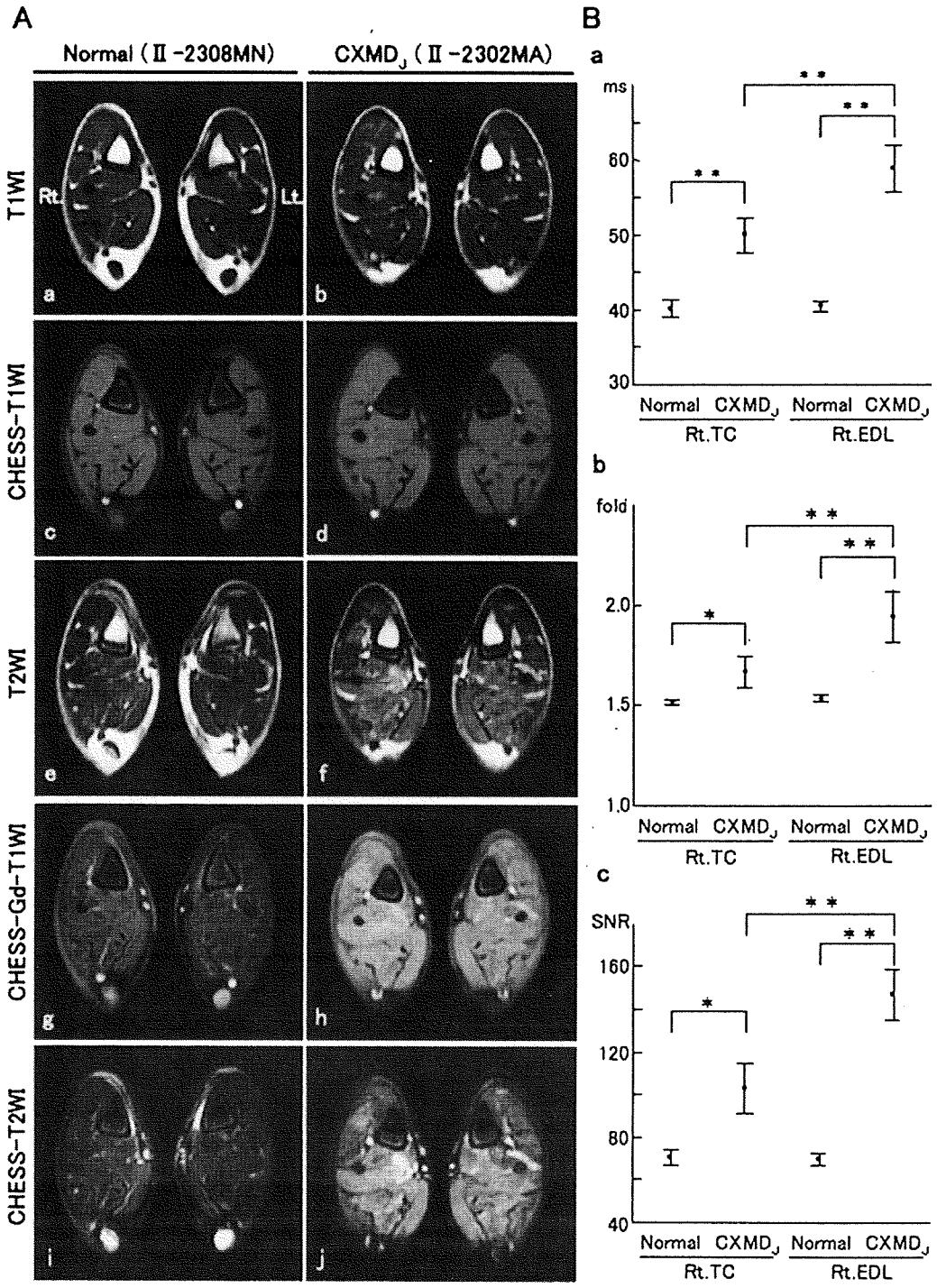

FIGURE 2. Cross-sectional MR images in lower leg muscles of 3-month-old normal and dystrophic dogs and comparison of three quantitative values in Rt. TC and Rt. EDL. **(A)** Representative images of normal (II-2308MN) and dystrophic (II-2302MA) dogs are shown. T1WI **(a, b)**, CHESS-T1WI **(c, d)**, T2WI **(e, f)**, CHESS-Gd-T1WI **(g, h)**, and CHESS-T2WI **(i, j)**. Rt, right side; Lt, left side. **(B)** Comparison of T2 relaxation time **(a)**, contrast enhancement (CE) **(b)**, and SNR of CHESS-T2WI **(c)** between three 3-month-old normal (II-2308MN, II/III-3911MN, and II-4202MN) and three littermate dystrophic (II-2302MA, II/III-3903MA, and II-4204MA) dogs are shown. Rt. TC, right side tibialis cranialis; Rt. EDL, right side extensor digitorum longus. Error bar: mean ± SD; $^*P < 0.05$; $^{**}P < 0.01$.

morphological changes of $CXMD_J$ lower leg muscles, we biopsied the Rt. TC and Rt. EDL of a normal dog (II-2308MN) and a $CXMD_J$ dog (II-2302MA) and carried out histopathological examinations. In TC of the $CXMD_J$, we found necrotic fibers, regenerating myofibers with central nuclei, a slight increase in cellular infiltration, and moderate variation in fiber size (Fig. 3A, c). Immunostaining with anti-IgG antibody, which is a marker for muscle necrosis,[37] revealed a slight degree of IgG uptake in the cytoplasm (Fig. 3A, d). On the other hand, EDL of the $CXMD_J$ showed many necrotic and hypercontracted fibers, severe cellular infiltration, and an increase in interstitial connective tissue (Fig. 3B, c). Moreover, the cytoplasm of this muscle showed a severe degree of IgG uptake (Fig. 3B, d). The necrotic and inflammatory changes in the muscle corresponded to the higher SNR on CHESS-T2W images.

MRI Findings of Lower Leg Muscles in a 7-year-old Normal Dog. Next, we obtained muscle images of a 7-year-old normal dog, 00-174MN (Fig. 4A). As shown in Figure 4A, a, c, e, g, and i, the lower leg muscles showed a homogeneous signal intensity in each sequence. Homogeneous but slight contrast enhancement was found on Gd-T1WI and CHESS-Gd-T1WI, as seen in 3-month-old normal dogs.

MRI Findings of Lower Leg Muscles in 7-Year-Old Dystrophic Dogs. We performed muscle MRI on two 7-year-old $CXMD_J$ dogs. II-C04MA showed muscle weakness and atrophy, gait disturbance, macroglossia, arthrogryposis, and dysphagia, but the dog could still rise and walk. Another dog, II-C12MA, was found to have difficulty in rising at the age of about 6.5 years. These two $CXMD_J$ showed mild clinical symptoms and signs despite their ages, which is sometimes seen in less affected GRMD.[8] We have previously reported that the clinical severity in Beagle-crossed dystrophic dogs was milder than that in GRMD,[14] in accordance with a separate report from another facility.[8]

MRI indicated muscle atrophy in both dogs, but the degree of muscle atrophy was more striking in II-C12MA than that in II-C04MA. Figure 4A, b, d, f, h, and j shows representative cross-sectional images of II-C04MA. On T1WI, almost all lower leg muscles of both dogs, in particular TC, EDL, and GC, revealed diffuse hyperintensity regions (Fig. 4A, b), although FHL and FDL did not show remarkable change compared with the normal dog. On CHESS-T1WI, these hyperintense regions were considerably suppressed, suggesting fat infiltration with progression of the disease (Fig. 4A, d), which was reported in a previous MRI study of DMD.[19]

On T2WI, II-C04MA showed slight and moderate hyperintensity in TC and other lower leg muscles, respectively (Fig. 4A, f). On the other hand, II-C12MA also had an area that showed remarkable T2 hyperintensity with T1 hyperintensity, but there is no area of T2 hyperintensity without T1 hyperintensity, with the exception of FHL (data not shown).

On CHESS-T2WI, FDL, GC, FHL, and FDS of II-C04MA and FHL of II-C12MA showed hyperintensity, but significant signal changes were found in neither TC of II-C04MA nor almost all lower leg muscles of II-C12MA (Fig. 4A, j, and data not shown).

On CHESS-Gd-T1WI of II-C04MA, the CHESS sequence considerably suppressed the hyperintense fat signal, but the contrast agent greatly enhanced the muscle regions left in all lower leg muscles, especially EDL, FHL, FDL, GC, and FDS (Fig. 4A, h). Contrast agent uptake was also found on CHESS-Gd-T1WI of II-C12MA, but the degree of uptake was lower than that of II-C04MA (data not shown).

Comparison of MR Signal Intensity in 7-Year-Old Normal and Dystrophic Dogs. To quantitatively assess the MRI findings of $CXMD_J$ dogs, we calculated the T2 relaxation time, CE, and SNR of CHESS-T2WI in TC of one 7-year-old normal dog and two $CXMD_J$ dogs. T2 relaxation time of TC was moderately prolonged in both $CXMD_J$ dogs (46.4 and 47.4 ms) when compared with that in a normal dog (37.0 ms) (Fig. 4B, a). Similarly, the effect of contrast enhancement was also increased in TC of each $CXMD_J$ (1.439- and 1.465-fold) relative to that of a normal dog (1.229-fold) (Fig. 4B, b). However, the SNR of CHESS-T2WI in TC of both $CXMD_J$ dogs (77.7 and 75.0) was not significantly increased when compared with that of a normal dog (74.7) (Fig. 4B, c). The discrepancy between the SNR of CHESS-T2WI and T2 relaxation times, and the effect of contrast enhancement should be carefully considered in the examination of affected skeletal muscle morphology.

Histopathological Findings in Lower Leg Muscles of 7-year-old Normal and Dystrophic Dogs. To determine the relationship between MRI findings and morphological changes in $CXMD_J$ lower leg muscles, we biopsied the Rt. TC of 00-174MN and

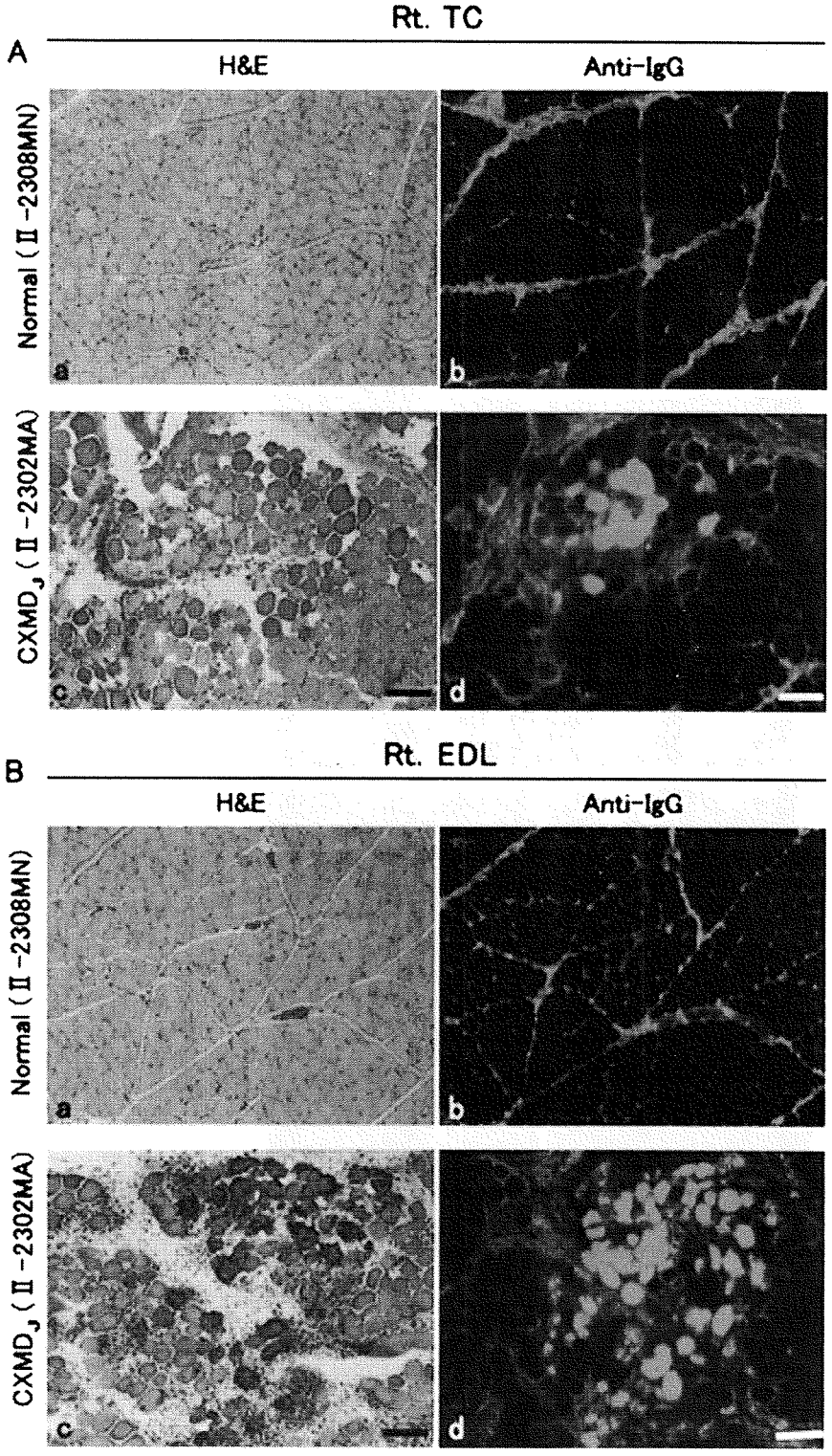

FIGURE 3. Histopathological examinations in Rt. TC and Rt. EDL of 3-month-old normal and dystrophic dogs.**(A)** Hematoxylin and eosin (H&E) staining **(a, c)** and IgG immunostaining **(b, d)** in Rt. TC of 3-month-old normal (II-2308MN) **(a, b)** and dystrophic (II-2302MA) dogs **(c, d)**. **(B)** H&E **(a, c)** and IgG immunostaining **(b, d)** in Rt. EDL of 3-month-old normal (II-2308MN) **(a, b)** and dystrophic (II-2302MA) dogs **(c, d)** are also shown. Bar = 100 μm.

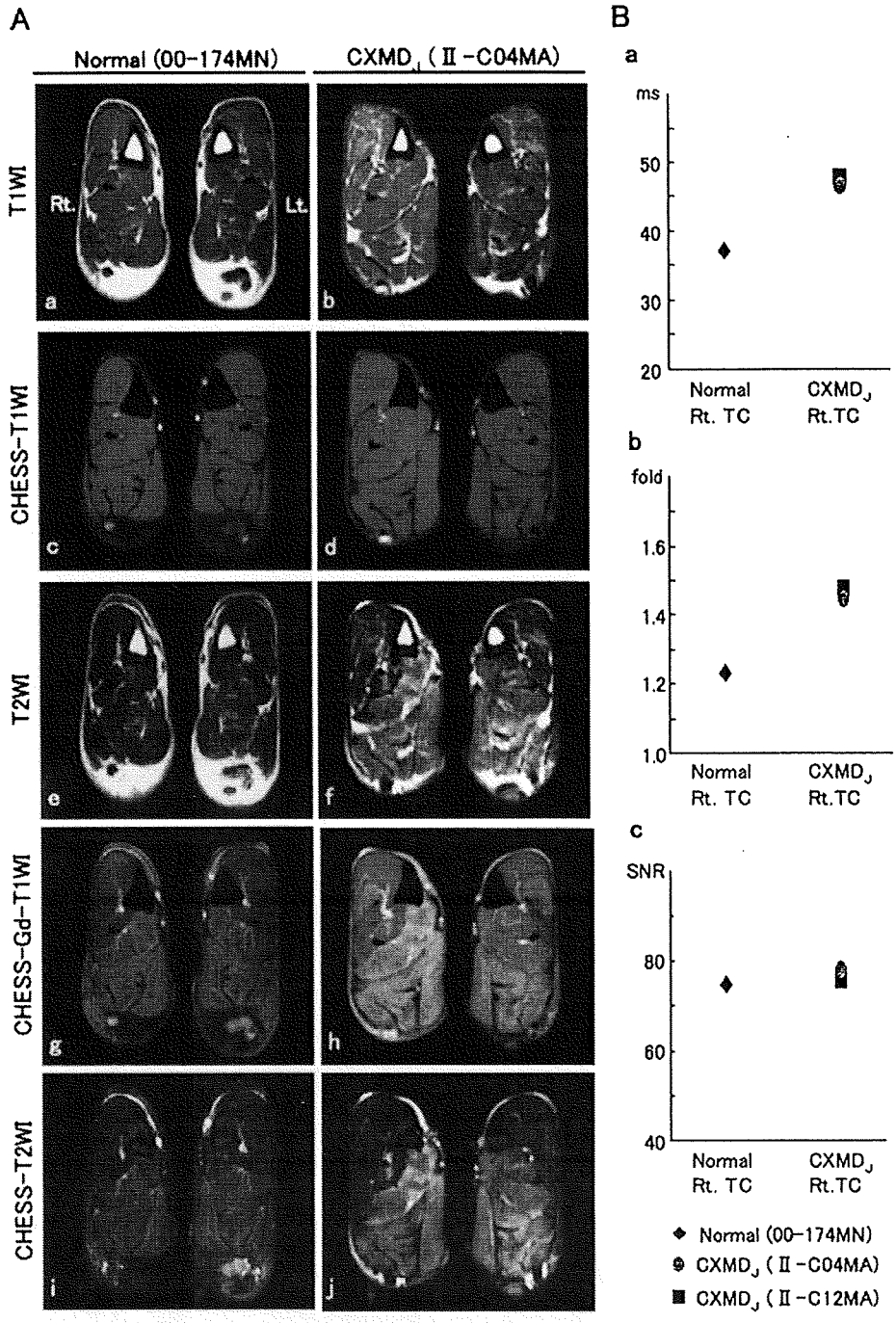

FIGURE 4. Cross-sectional MRI of lower leg muscles of 7-year-old normal and dystrophic dogs and comparison of three quantitative values in Rt. TC. **(A)** Representative images of 7-year-old normal (00-174MN) and dystrophic (II-C04MA) dogs are shown. T1WI **(a, b)**, CHESS-T1WI **(c, d)**, T2WI **(e, f)**, CHESS-Gd-T1WI **(g, h)**, and CHESS-T2WI **(i, j)**. Rt, right side; Lt, left side. **(B)** Comparisons of T2 relaxation time **(a)**, contrast enhancement (CE) **(b)**, and CHESS-T2W SNR **(c)** between the muscles in 7-year-old normal (00-174MN) and dystrophic (II-C04MA and II-C12MA) dogs are shown. TC, tibialis cranialis.

II-C04MA and carried out histopathological examinations. In CXMD$_J$ dogs, we found a few degenerated and many regenerated fibers with central nuclei and a moderate degree of fiber size variation together with fibrotic changes (Fig. 5d). IgG accumulation was found in only a few fibers, but it was extensively distributed in the interstitial tissues (Fig. 5e). Oil red O staining revealed definite fatty infiltration in the CXMD$_J$ dogs (Fig. 5f).

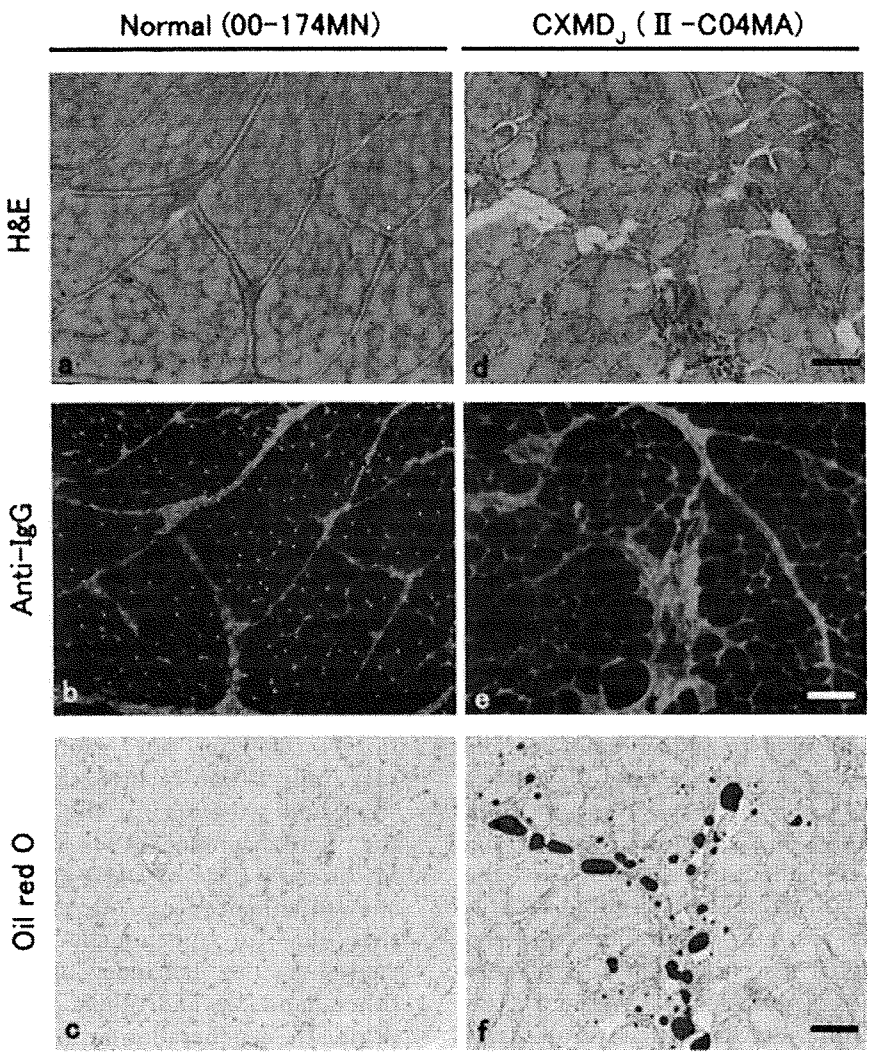

FIGURE 5. Histopathology in Rt. TC of 7-year-old normal and dystrophic dogs. We performed hematoxylin and eosin (H&E) staining **(a, d)**, IgG immunostaining **(b, e)**, and oil red O staining **(c, f)** on tissues of 7-year-old normal (00-174MN) **(a–c)** and dystrophic (II-C04MA) dogs **(d–f)**. Bar = 100 μm.

DISCUSSION

Previous studies have attempted to noninvasively evaluate involvement of striated muscle in DMD patients or the animal models by various MRI sequences; however, a method for more accurate and precise assessment of acute-phase responses such as muscle necrosis and/or inflammation is necessary, because it is difficult to distinguish between these lesions and fat infiltration and/or fibrosis by conventional MRI sequences. Among dystrophic processes, especially in muscle necrosis, the intramuscular water concentration and extracellular components are increased, with the water imbalance having been induced by the deficiency of sarcolemmal membrane integrity.[19,26,38] CHESS-T2WI may be one of the tools to solve this problem, because the sequence can selectively cancel fat tissue signals.

CHESS-T2WI Is Useful to Evaluate Dystrophic Skeletal Muscle Involvement in Early Stage. First, we tried to detect necrotic and/or inflammatory lesions in the early stage of CXMD$_J$ by using a CHESS-T2WI sequence. EDL of a 3-month-old CXMD$_J$ dog showed massive and severe necrosis and inflammatory cell infiltration in the pathological analyses, but TC of the dog revealed localized and moderate necrosis and inflammation. The SNR of CHESS-T2WI in EDL showed a significant increase compared with that in TC. These findings suggest that there is a correlation between SNR of CHESS-T2WI and the degree of necrotic and inflamma-

tory changes in the histopathology. Moreover, the SNR of CHESS-T2WI was consistent with T2 relaxation time or contrast enhancement in the early stage of muscular dystrophy. Previous contrast agent studies sensitively detected early dystrophic muscle involvement that showed the increase of cell membrane permeability.[24,25] In the forelegs of 2-month-old GRMD dogs, the maximum relative enhancement, which was calculated from fat-saturated T1-weighted images pre- and post-gadolinium injection, was almost doubled compared with normal control dogs.[39] However, side effects of the contrast agent itself or cytotoxicity may be of concern, because influx of the contrast agent into damaged muscle fibers occurred. CHESS-T2WI can identify dystrophic lesions without a contrast agent and may facilitate more sensitive and clearer optical evaluation of early dystrophic lesions than other fat suppression sequences, because the SNR on either STIR or the multipoint Dixon technique is lower than that on CHESS.[40]

CHESS-T2WI May Be Able to Differentiate Necrotic and/or Inflammatory Changes from Fatty Changes in Advanced Stage of Dystrophic Dogs. Next, we studied whether CHESS-T2WI is able to evaluate necrotic and/or inflammatory lesions in the advanced stage of $CXMD_J$. TC of 7-year-old $CXMD_J$ dogs showed severe fatty infiltration and an increase in interstitial tissues without necrosis and inflammation. The SNR of CHESS-T2WI in TC was not significantly different from that of the age-matched normal dog, suggesting that CHESS-T2WI is a good tool to evaluate necrotic and/or inflammatory changes, even though extensive fatty infiltration exists. On the other hand, the T2 relaxation time and enhancing effect of the contrast agent were increased, although necrotic and inflammatory changes were not present. It is possible that the prolongation of T2 relaxation time or the increase of contrast enhancement is affected by fatty infiltration, increase of interstitium, and/or microvascular flow, and therefore necrotic and inflammatory changes could be overestimated by these sequences and indexes. CHESS-T2WI may reflect necrotic lesions more precisely in the intermediate to advanced stage without special contrast agents, because the SNR of CHESS-T2WI was elevated in EDL of II-C04MA, where it is thought that necrotic and fatty changes coexist (data not shown). On the other hand, it is also important to evaluate fatty infiltration in the advanced stages of DMD. In a recent study, the percentage of intramuscular fat tissue was measured by three-point Dixon MRI, which may accurately reflect the clinical severity of DMD patients.[41]

Muscle Regeneration in Advanced Stage of $CXMD_J$ May Stabilize Cell Membrane. We found that the majority of muscle fibers in TC of 7-year-old $CXMD_J$ dogs were composed of regenerated fibers with central nuclei, but those fibers did not show IgG uptake, in accordance with the lack of abnormal signals on CHESS-T2WI at this stage. The histopathological findings and muscle physiological functions were ameliorated at the advanced stage in *mdx* mice compared with those in the early stage.[9] Moreover, studies using 31-phosphorus magnetic resonance spectroscopy (^{31}P-MRS) demonstrated biochemical abnormalities in the regulations of intracellular ion and oxidative metabolism of dystrophic muscles at the early stage.[42–45] It was, however, reported that older GRMD (>30 months) did not demonstrate further increases in the inorganic phosphate (Pi) to phosphocreatine (PCr) ratio [Pi/(Pi+PCr)] after exercise, and these results may reflect the relative stabilization of clinical signs and symptoms at the later stage, as far as they were examined by ^{31}P-MRS.[45] Skeletal muscle in the early stage of DMD and the model animals showed enhanced necrotic and regeneration activities due to functionally defective regulation caused by the deficiency of dystrophin. On the other hand, we and others found a lower degree of muscle degeneration at the advanced stage, suggesting some degree of membrane stability remains in regenerated fibers, resulting in resistance to further necrosis. Retention of membrane stability in the advanced stage may be related to the shift of muscle fiber types from fast to slow[46] and/or compensatory expression of utrophin,[47] a homolog of dystrophin.

One of the limitations of the CHESS sequence is that it requires a presaturation pulse. Fat suppression by the CHESS sequence is not applicable with a low magnetic field (<1.5 T), because dispersion of the frequency direction between water and fat depends on the main magnetic field.[48] Another limitation is that CHESS-T2WI does not allow evaluation of fibrotic changes. We, however, suggest that CHESS-T2WI could precisely and perceptively provide much information, such as the presence and severity of necrotic and inflammatory changes throughout all stages of the disease. Moreover, CHESS-T2WI is safer than other conventional sequences, because the sequence does not require

contrast agent enhancement. CHESS-T2WI may be useful to understand the pathological findings, to monitor therapeutic effects in clinical trials, and to predict functional recovery in muscular dystrophies such as DMD.

This study was supported by Health Sciences Research Grants for Research on Psychiatric and Neurological Diseases and Mental Health (H12-kokoro-025, H15-kokoro-021, H18-kokoro-019), Human Genome and Gene Therapy (H13-genome-001, H16-genome-003), and Health and Labor Sciences Research Grants for Translation Research (H19-translational research-003) from the Ministry of Health, Labor and Welfare of Japan, and Grants-in-Aid for Scientific Research from the Ministry of Education, Science, Sports and Culture of Japan (to S.T.). The authors thank Hideki Kita, Shin'ichi Ichikawa, Yumiko Yahata, Takayuki Nakayama, Masayoshi Sawada, and Kazue Kinoshita (JAC, Inc., Tokyo) for maintenance of the dogs, and Ryoko Nakagawa and Satoru Masuda (Department of Molecular Therapy, National Institute of Neuroscience, NCNP, Tokyo) for their technical assistance. We also thank Dr. Hironaka Igarashi (Center for Integrated Human Brain Science, Niigata University) for technical advice concerning MRI.

REFERENCES

1. Moser H. Duchenne muscular dystrophy: pathogenetic aspects and genetic prevention. Hum Genet 1984;66: 17–40.
2. Koenig M, Hoffman EP, Bertelson CJ, Monaco AP, Feener C, Kunkel LM. Complete cloning of the Duchenne muscular dystrophy (DMD) cDNA and preliminary genomic organization of the DMD gene in normal and affected individuals. Cell 1987;50:509–517.
3. Campbell KP. Three muscular dystrophies: loss of cytoskeleton–extracellular matrix linkage. Cell 1995;80:675–679.
4. Ervasti JM, Ohlendieck K, Kahl SD, Gaver MG, Campbell KP. Deficiency of a glycoprotein component of the dystrophin complex in dystrophic muscle. Nature 1990;345:315–319.
5. Cullen MJ, Mastaglia FL. Morphological changes in dystrophic muscle. Br Med Bull 1980;36:145–152.
6. Marden FA, Connolly AM, Siegel MJ, Rubin DA. Compositional analysis of muscle in boys with Duchenne muscular dystrophy using MR imaging. Skel Radiol 2005;34:140–148.
7. Coulton GR, Morgan JE, Partridge TA, Sloper JC. The mdx mouse skeletal muscle myopathy: I. A histological, morphometric and biochemical investigation. Neuropathol Appl Neurobiol 1988;14:53–70.
8. Valentine BA, Cooper BJ, de Lahunta A, O'Quinn R, Blue JT. Canine X-linked muscular dystrophy. An animal model of Duchenne muscular dystrophy: clinical studies. J Neurol Sci 1988;88:69–81.
9. Muntoni F, Mateddu A, Marchei F, Clerk A, Serra G. Muscular weakness in the mdx mouse. J Neurol Sci 1993;120: 71–77.
10. Tanabe Y, Esaki K, Nomura T. Skeletal muscle pathology in X chromosome-linked muscular dystrophy (mdx) mouse. Acta Neuropathol (Berl) 1986;69:91–95.
11. Cooper BJ, Winand NJ, Stedman H, Valentine BA, Hoffman EP, Kunkel LM, et al. The homologue of the Duchenne locus is defective in X-linked muscular dystrophy of dogs. Nature 1988;334:154–156.
12. Valentine BA, Cooper BJ, Cummings JF, de Lahunta A. Canine X-linked muscular dystrophy: morphologic lesions. J Neurol Sci 1990;97:1–23.
13. Shimatsu Y, Katagiri K, Furuta T, Nakura M, Tanioka Y, Yuasa K, et al. Canine X-linked muscular dystrophy in Japan (CXMDJ). Exp Anim 2003;52:93–97.
14. Shimatsu Y, Yoshimura M, Yuasa K, Urasawa N, Tomohiro M, Nakura M, et al. Major clinical and histopathological characteristics of canine X-linked muscular dystrophy in Japan, CXMDJ. Acta Myol 2005;24:145–154.
15. Yugeta N, Urasawa N, Fujii Y, Yoshimura M, Yuasa K, Wada MR, et al. Cardiac involvement in beagle-based canine X-linked muscular dystrophy in Japan (CXMDJ): electrocardiographic, echocardiographic, and morphologic studies. BMC Cardiovasc Disord 2006;6:47.
16. Liu M, Chino N, Ishihara T. Muscle damage progression in Duchenne muscular dystrophy evaluated by a new quantitative computed tomography method. Arch Phys Med Rehabil 1993;74:507–514.
17. Shimizu J, Matsumura K, Kawai M, Kunimoto M, Nakano I. X-ray CT of Duchenne muscular dystrophy skeletal muscles—chronological study for five years [in Japanese]. Rinsho Shinkeigaku 1991;31:953–959.
18. Mercuri E, Pichiecchio A, Allsop J, Messina S, Pane M, Muntoni F. Muscle MRI in inherited neuromuscular disorders: past, present, and future. J Magn Reson Imaging 2007;25: 433–440.
19. Huang Y, Majumdar S, Genant HK, Chan WP, Sharma KR, Yu P, et al. Quantitative MR relaxometry study of muscle composition and function in Duchenne muscular dystrophy. J Magn Reson Imaging 1994;4:59–64.
20. Schreiber A, Smith WL, Ionasescu V, Zellweger H, Franken EA, Dunn V, et al. Magnetic resonance imaging of children with Duchenne muscular dystrophy. Pediatr Radiol 1987;17:495–497.
21. McIntosh LM, Baker RE, Anderson JE. Magnetic resonance imaging of regenerating and dystrophic mouse muscle. Biochem Cell Biol 1998;76:532–541.
22. Matsumura K, Nakano I, Fukuda N, Ikehira H, Tateno Y, Aoki Y. Proton spin-lattice relaxation time of Duchenne dystrophy skeletal muscle by magnetic resonance imaging. Muscle Nerve 1988;11:97–102.
23. Dunn JF, Zaim-Wadghiri Y. Quantitative magnetic resonance imaging of the mdx mouse model of Duchenne muscular dystrophy. Muscle Nerve 1999;22:1367–1371.
24. Amthor H, Egelhof T, McKinnell I, Ladd ME, Janssen I, Weber J, et al. Albumin targeting of damaged muscle fibres in the mdx mouse can be monitored by MRI. Neuromuscul Disord 2004;14:791–796.
25. Straub V, Donahue KM, Allamand V, Davisson RL, Kim YR, Campbell KP. Contrast agent-enhanced magnetic resonance imaging of skeletal muscle damage in animal models of muscular dystrophy. Magn Reson Med 2000;44:655–659.
26. Walter G, Cordier L, Bloy D, Sweeney HL. Noninvasive monitoring of gene correction in dystrophic muscle. Magn Reson Med 2005;54:1369–1376.
27. Burstein D, Taratuta E, Manning WJ. Factors in myocardial "perfusion" imaging with ultrafast MRI and Gd-DTPA administration. Magn Reson Med 1991;20:299–305.
28. Baxter AB, Lazarus SC, Brasch RC. In vitro histamine release induced by magnetic resonance imaging and iodinated contrast media. Invest Radiol 1993;28:308–312.
29. Nomura M, Takeshita G, Katada K, Nakamura M, Kizukuri T, Ogura Y, et al. A case of anaphylactic shock following the administration of Gd-DTPA [in Japanese]. Nippon Igaku Hoshasen Gakkai Zasshi 1993;53:1387–1391.
30. Krinsky G, Rofsky NM, Weinreb JC. Nonspecificity of short time inversion recovery (STIR) as a technique of fat suppression: pitfalls in image interpretation. AJR Am J Roentgenol 1996;166:523–526.
31. Scarabino T, Giannatempo GM, Popolizio T, Scarale MG, Cammisa M, Salvolini U. Fast spin echo imaging of vertebral metastasis: comparison of fat suppression techniques (FSE-CHESS, STIR-FSE) [in Italian]. Radiol Med (Torino) 1996; 92:180–185.
32. Drevelegas A, Pilavaki M, Chourmouzi D. Lipomatous tumors of soft tissue: MR appearance with histological correlation. Eur J Radiol 2004;50:257–267.

33. Galant J, Marti-Bonmati L, Saez F, Soler R, Alcala-Santaella R, Navarro M. The value of fat-suppressed T2 or STIR sequences in distinguishing lipoma from well-differentiated liposarcoma. Eur Radiol 2003;13:337–343.
34. Morimoto Y, Tanaka T, Masumi S, Tominaga K, Shibuya T, Kito S, et al. Significance of frequency-selective fat saturation T2-weighted MR images for the detection of bone marrow edema in the mandibular condyle. Cranio 2004;22:115–123.
35. Cook LL, Foster PJ, Karlik SJ. Pathology-guided MR analysis of acute and chronic experimental allergic encephalomyelitis spinal cord lesions at 1.5T. J Magn Reson Imaging 2005; 22:180–188.
36. Bonny JM, Zanca M, Boespflug-Tanguy O, Dedieu V, Joandel S, Renou JP. Characterization in vivo of muscle fiber types by magnetic resonance imaging. Magn Reson Imaging 1998;16:167–173.
37. Straub V, Rafael JA, Chamberlain JS, Campbell KP. Animal models for muscular dystrophy show different patterns of sarcolemmal disruption. J Cell Biol 1997;139:375–385.
38. Mattila KT, Lukka R, Hurme T, Komu M, Alanen A, Kalimo H. Magnetic resonance imaging and magnetization transfer in experimental myonecrosis in the rat. Magn Reson Med 1995;33:185–192.
39. Thibaud JL, Monnet A, Bertoldi D, Barthelemy I, Blot S, Carlier PG. Characterization of dystrophic muscle in golden retriever muscular dystrophy dogs by nuclear magnetic resonance imaging. Neuromuscul Disord 2007;17:575–584.
40. Mao J, Yan H, Brey WW, Bidgood WD Jr, Steinbach JJ, Mancuso A. Fat tissue and fat suppression. Magn Reson Imaging 1993;11:385–393.
41. Wren TA, Bluml S, Tseng-Ong L, Gilsanz V. Three-point technique of fat quantification of muscle tissue as a marker of disease progression in Duchenne muscular dystrophy: preliminary study. AJR Am J Roentgenol 2008;190:W8–12.
42. Dunn JF, Tracey I, Radda GK. A 31P-NMR study of muscle exercise metabolism in mdx mice: evidence for abnormal pH regulation. J Neurol Sci 1992;113:108–113.
43. Dunn JF, Tracey I, Radda GK. Exercise metabolism in Duchenne muscular dystrophy: a biochemical and [31P]-nuclear magnetic resonance study of mdx mice. Proc Biol Sci 1993; 251:201–206.
44. Le Rumeur E, Le Tallec N, Lewa CJ, Ravalec X, de Certaines JD. In vivo evidence of abnormal mechanical and oxidative functions in the exercised muscle of dystrophic hamsters by 31P-NMR. J Neurol Sci 1995;133:16–23.
45. McCully K, Giger U, Argov Z, Valentine B, Cooper B, Chance B, et al. Canine X-linked muscular dystrophy studied with in vivo phosphorus magnetic resonance spectroscopy. Muscle Nerve 1991;14:1091–1098.
46. Yuasa K, Nakamura A, Hijikata T, Takeda S. Dystrophin deficiency in canine X-linked muscular dystrophy in Japan (CXMDJ) alters myosin heavy chain expression profiles in the diaphragm more markedly than in the tibialis cranialis muscle. BMC Musculoskel Disord 2008;9:1.
47. Hirst RC, McCullagh KJ, Davies KE. Utrophin upregulation in Duchenne muscular dystrophy. Acta Myol 2005;24: 209–216.
48. Haase A, Frahm J, Hanicke W, Matthaei D. 1H NMR chemical shift selective (CHESS) imaging. Phys Med Biol 1985;30: 341–344.

Neuropathology 2009; **29**, 494–501 doi:10.1111/j.1440-1789.2009.01028.x

Symposium: Clinicopathological aspects of neuromuscular disorders – A new horizon

Exon-skipping therapy for Duchenne muscular dystrophy

Akinori Nakamura and Shin'ichi Takeda

Department of Molecular Therapy, National Institute of Neuroscience, National Center of Neurology and Psychiatry (NCNP), Ogawa-higashi, Kodaira, Tokyo, Japan

Duchenne muscular dystrophy (DMD) is a lethal muscle disorder caused by mutations in the *DMD* gene for which no mutation-targeted therapy has been available thus far. However, exon-skipping mediated by antisense oligonucleotides (AOs), which are short single-strand DNAs, has considerable potential for DMD therapy, and clinical trials in DMD patients are currently underway. This exon-skipping therapy changes an out-of-frame mutation into an in-frame mutation, aiming at conversion of a severe DMD phenotype into a mild phenotype by restoration of truncated dystrophin expression. Recently, stable and less-toxic AOs have been developed, and their higher efficacy was confirmed in mice and dog models of DMD. In this review, we briefly summarize the genetic basis of DMD and the potential and perspectives of exon skipping as a promising therapy for this disease.

Key words: antisense oligonucleotide, DMD animal model, *DMD* gene, Duchenne muscular dystrophy (DMD), dystrophin, exon skipping.

INTRODUCTION

Muscular dystrophy is a group of disorders that shows progressive muscle atrophy and weakness and the histopathology of which reveals degeneration and regeneration of muscle fibers. Among them, Duchenne muscular dystrophy (DMD), an X-linked disorder, is the most common and produces the most severe phenotype. This disorder manifests around the age 2–5 years by difficulty in walking, and the skeletal muscle involvement is progressive, resulting in patients being wheelchair-bound by the age of 13. The patients die of cardiac or respiratory failure due to dilated cardiomyopathy around the age of 30 years, at least in Japan. The responsible gene, *DMD*, encodes dystrophin, which is expressed at the sarcolemma of muscle fibers, and *DMD* mutations interrupt the reading-frame, resulting in a complete loss of dystrophin expression, which causes DMD.[1] The histopathology shows degeneration, necrosis, inflammatory cell invasion, and regeneration of muscle fibers, which are eventually replaced by fibrous connective and fat tissue. Besides DMD, two phenotypes of the dystrophin-deficient condition, Becker muscular dystrophy (BMD) and X-linked dilated cardiomyopathy (XLDCM) are known. BMD is a milder variant of DMD, and XLDCM shows dilated cardiomyopathy without overt skeletal muscle signs and symptoms. All three phenotypes of dystrophin deficiency are called dystrophinopathies.

Several therapeutic strategies for treatment of DMD have been investigated extensively: gene therapy using micro-dystrophin with an adeno-associated virus (AAV) vector,[2] stem cell transplantation using muscle satellite cells[3] or bone marrow stromal cells,[4] and read-through therapy for nonsense mutations.[5] However, an effective treatment has not yet been established. In recent years, exon skipping using antisense oligonucleotides (AOs) has been considered one of the therapeutic strategies for restoration of dystrophin expression at the sarcolemma. AOs are artificial nucleic acids that recognize a specific sequence of the mRNA, resulting in a change in the splicing pattern or translation. Currently, various AOs possessing the properties of high stability, high efficacy and low toxicity, have been developed. Here, we review advances in exon-skipping therapy for DMD.

THE *DMD* GENE AND ITS MUTATION

The *DMD* gene is located on the human chromosome Xp2.1, and it is the largest gene in the human genome, with

Correspondence: Shin'ichi Takeda, MD, PhD, Department of Molecular Therapy, National Institute of Neuroscience, National Center of Neurology and Psychiatry (NCNP), 4-1-1 Ogawa-higashi, Kodaira, Tokyo 187-8502, Japan. Email: takeda@ncnp.go.jp

Received 30 January 2009 and accepted 22 March 2009; published online 22 May 2009.

79 exons spanning more than 2500 kb. The *DMD* gene encodes a product called dystrophin. Full-length dystrophin mRNA is about 14 kb and is mainly expressed in skeletal, cardiac and smooth muscles, and the brain. Dystrophin is a rod-shape structure that consists of four domains: (i) the N-terminal actin-binding domain; (ii) a rod domain composed of 24 spectrin-like rod repeats and 4 hinges; (iii) a cysteine-rich domain that interacts with dystroglycan and sarcoglycan complexes; and (iv) the C-terminal domain that interacts with the syntrophin complex and dystrobrevin. Dystrophin is localized at the sarcolemma and forms a dystrophin-glycoprotein complex (DGC) with dystroglycan, sarcoglycan, and syntrophin/dystrobrevin complexes. Then, DGC links the cytoskeletal protein actin to the basal lamina of muscle fibers. DGC is considered to work as a membrane stabilizer during muscle contraction or a transducer of signals from the extracellular matrix to the muscle cytoplasm via its interactions with intracellular signaling molecules.[6] Dystrophin deficiency leads to a condition in which the membrane is leaky under mechanical or hypo-osmotic stress. Consequently, Ca^{2+} permeability is increased, and various Ca^{2+}-dependent proteases, such as calpain, are activated in dystrophin deficiency. It has also been proposed that alteration of the expression or function of the plasma membrane proteins associated with dystrophin, such as neuronal nitric oxide synthase (nNOS), aquaporin-4, Na^+ channel, L-type Ca^{2+} channel, and stretch-activated channel, are involved in the molecular mechanisms of muscle degeneration.[6]

In DMD patients, various mutations in the *DMD* gene, such as missense, nonsense, deletion, insertion, or duplication, have been identified (http://www.hgmd.org). In general, when the reading-frame of amino acids is disrupted by a mutation (out-of-frame), dystrophin is not expressed, resulting in the severe phenotype of DMD. On the other hand, when the reading-frame is maintained despite the existence of a mutation (in-frame), a truncated but still functional dystrophin is expressed, leading to the more benign phenotype of Becker muscular dystrophy (BMD). Ninety-two percent of the DMD/BMD phenotypes are explained by the "frame-shift theory." In the *DMD* gene, there are two hot spots for mutation: around exons 3–7 and exons 45–55.

RATIONALE OF EXON-SKIPPING THERAPY IN DMD

In DMD, dystrophin is basically absent at the sarcolemma, although some dystrophin-positive fibers, which are called revertant fibers, are detected in DMD patients and DMD animal models. The number of revertant fibers increases with age due to the cycle of degeneration and regeneration.[7,8] It is currently thought that the molecular mechanism underlying revertant fibers is the skipping of exon(s) around the original mutation, which gives rise to correction of the reading frame and expression of dystrophin at the sarcolemma.[9] Consequently, exon skipping has attracted attention as a strategy for restoration of dystrophin expression in DMD.[8–10] In addition, exon-skipping therapy for DMD has been advanced by the development of several new AOs.[11] Exon-skipping therapy has been reported to be practical for up to 90% of DMD patients having a deletion mutation.[12,13] In addition, the ethical issues involved in exon-skipping therapy are fewer in number than those in gene therapy or stem-cell transplantation therapy because AOs are classified as a drug rather than a gene therapy agent by the Food and Drug Administration (FDA) of the USA and representative agencies in the EU and Japan. Based on reports that asymptomatic patients with high blood creatine kinase concentrations have an in-frame deletion in the *DMD* gene,[14,15] it is possible that exon-skipping therapy could convert DMD phenotype to an asymptomatic phenotype rather than the milder phenotype of dystrophin deficiency, BMD.

DEVELOPMENT OF ANTISENSE OLIGONUCLEOTIDE AND DESIGN OF SEQUENCE

Antisense oligonucleotides are chemically synthesized 20–25 base-long single-strand DNAs that are designed to hybridize with a complementary sequence in the target mRNA. In 1989, Isis Pharmaceuticals developed the AO drug Vitravene (fomivirsen) for retinitis due to cytomegalovirus infection in AIDS patients, and it was the first AO approved by the FDA. However, the clinical application did not go smoothly because of adverse effects such as inflammation, and it was terminated in 1999.

Various chemistries for AOs have been proposed to overcome the unstable nature of single-strand DNA or RNA molecules (Fig. 1). Several modifications of AOs include a bicyclic-locked nucleic acid (LNA), peptide nucleic acid (PNA), ethylene-bridged nucleic acid (ENA), 2′-O-methyl phosphorothionate AO (2OMeAO), phosphorodiamidate morpholino oligomer (PMO: morpholino), and peptide-linked PMO (PPMO).[16,17] Development of appropriate AOs requires consideration of several characteristics of AOs, such as the chemical specificity, affinity, nuclease resistance, stability, safety, and ease of synthesis,[16,18] but among them, 2OMeAO and PMO are the most frequently utilized because of their suitable properties.

The structure of 2OMeAO is similar to that of RNA, but it has been methylated at the 2′-OH position of the ribose ring. 2OMeAO is widely used because it is relatively cheap to produce and easy to synthesize, has high stability and